Electrospun medicated shellac nanofibers for colon-targeted drug delivery

Xia Wang[1]
Deng-Guang Yu[1]
Xiao-Yan Li[1]
Annie Bligh[2]
Gareth R. Williams[3]

[1] School of Materials Science & Engineering, University of Shanghai for Science and Technology, China
[2] Faculty of Science and Technology, University of Westminster, UK
[3] UCL School of Pharmacy, UCL, UK

Electrospun Medicated Shellac Nanofibers for Colon-targeted Drug Delivery

Xia Wang[a], Deng-Guang Yu[a,*], Xiao-Yan Li[a],
SW Annie Bligh[b], Gareth R. Williams[c,*]

[a] School of Materials Science & Engineering, University of Shanghai for Science and Technology, 516 Jungong Road, Shanghai 200093, China.
[b] Faculty of Science and Technology, University of Westminster, 115 New Cavendish Street, London W1W 6UW, UK.
[c] UCL School of Pharmacy, University College London, 29-39 Brunswick Square, London WC1N 1AX, UK.

* **Corresponding authors:**
Prof. Deng-Guang Yu and Dr. Gareth R. Williams

Tel: +86-21-55270632 (D-GY); +44-207-7535868 (GRW)
Fax: +86-21-55270632 (D-GY); +44-207-753 5942 (GRW)
Email: ydg017@usst.edu.cn (D-GY); g.williams@ucl.ac.uk (GRW)

Abstract: Medicated shellac nanofibers providing colon-specific sustained release were fabricated using coaxial electrospinning. A mixed solution of 75% (w/v) shellac and 15% (w/v) ferulic acid (FA) in ethanol was used as the core fluid, and a mixture of ethanol and N,N-dimethylformamide (8/10 v/v) as the shell. The presence of the shell fluid was required to prevent frequent clogging of the spinneret. The diameters of the fibers (*D*) can be manipulated by varying the ratio of shell to core flow rates (*F*), according to the equation $D=0.52F^{-0.19}$. Scanning electron microscopy images revealed that fibers prepared with *F* values of 0.1 and 0.25 had linear morphologies with smooth surfaces, but when the shell fluid flow rate was increased to 0.5 the fiber integrity was compromised. FA was found to be amorphously distributed in the fibers on the basis of X-ray diffraction and differential scanning calorimetry results. This can be attributed to good compatibility between the drug and carrier: IR spectra indicated the presence of hydrogen bonds between the two. *In vitro* dissolution tests demonstrated that there was minimal FA release at pH 2.0, and sustained release in a neutral dissolution medium. The latter occurred through an erosion mechanism. During the dissolution processes, the shellac fibers were gradually converted into nanoparticles as the FA was freed into solution, and ultimately completely dissolved.

Keywords: Medicated nanofibers; Colon-targeted release; Coaxial electrospinning; Erosion mechanism; Shellac

1. Introduction

Over the last decades, a wide variety of different materials have been considered as carriers for drug delivery systems. These include both synthetic polymers and macromolecules extracted from natural products, such as proteins and polysaccharides (Allen and Cullis, 2004; Liu et al., 2008). Shellac, a resin secreted by the female lac beetle, is one material to have attracted much attention for biomedical applications (Limmatvapirat et al., 2008; Limmatvapirat et al., 2007). These polymers have been processed by a broad gamut of technologies with the aim of preparing advanced drug delivery systems (DDS), with nanotechnologies being particularly popular (Farokhzad, 2008; Hubbell and Chikoti, 2012). Because of the convenience and high patient compliance associated with oral administration, nanotechnology has been widely explored in this content (Pouton and Porter, 2008).

Nanoscale products have shown particular potential for the effective oral delivery of poorly water-soluble active ingredients. This is because nanoscale products have large surface-area-to-volume ratios and thus, if solid solutions (or suspensions) of a drug in a carrier can be prepared, it is facile to accelerate dissolution rate and enhance solubility (Merisko-Liversidge and Liversidge, 2011). There are a range of approaches which can be used to prepare nanoscale DDS, which can broadly be classified as “top down” or “bottom up”. Of the former, electrospinning has proven popular for generating medicated nanofibers; these one-dimensional systems have been widely studied for application as a broad range of DDS, including for oral

85 administration. Importantly, electrospinning has the ability to be moved to large-scale
86 production (Vrbata et al., 2014; Nagy et al., 2015). Medicated nanofibers are
87 fabricated from a mixed solution or melt comprising a carrier polymer and the desired
88 active ingredient; these are most commonly processed using single fluid
89 electrospinning (Paaver et al., 2015; Balogh et al., 2015).

90 Around one hundred polymers have been successfully electrospun into fibers
91 (Sun et al., 2014). Among these, more than ten are frequently spun with active
92 pharmaceutical ingredients to create medicated fibers – for instance,
93 poly(vinylpyrrolidone), ethyl cellulose, and chitosan (Yu et al., 2013). In general,
94 natural polymers have been more widely studied than synthetic materials for oral drug
95 delivery (Sridhar et al., 2015). Proteins including collagen (Zhang et al., 2013), silk
96 fibroin (Dinis et al., 2014), keratin (Mogosanu et al., 2014; Edwards et al., 2015),
97 gelatin (Baigvera et al., 2014), and polysaccharides such as chitosan (Lin et al., 2013),
98 alginate (Ma et al., 2012), and cellulose and its derivatives (Kai et al., 2015) have all
99 been electrospun and explored for drug delivery systems.

100 Colon-targeted drug delivery is attractive not only for local delivery to treat
101 diseases of the colon, but also for improving the bioavailability of poorly
102 water-soluble drugs as a result of the long retention time and high colonic surface area
103 (Vats and Pathak, 2013). Shellac is insoluble in the stomach, and thus has proved to
104 be useful as a drug carrier for colon-targeted delivery in traditional formulation
105 approaches (Ravi et al., 2008). Shellac-coated tablets are ubiquitous in the pharmacy,
106 and new developments in this area are still being explored (Rachmawati et al., 2012):

in one recent example, Henning et al. investigated the use of shellac to coat liquid-filled pectinate capsules and target delivery to the colon (Henning et al., 2012).

In this work, for the first time, colon-targeting shellac nanofibers loaded with the anti-oxidant phytochemical ferulic acid were created using a coaxial electrospinning process. The sheath fluid comprised a mixture of ethanol and dimethylformamide, while the core contained the polymer and active ingredient. The influence of the shell solvent flow rate on fiber formation and the drug release mechanism were studied.

2. Materials and methods

2.1. Materials

Shellac (95% purity, wax free) was obtained from the Shanghai Wanjiang Bio-Technology Co., Ltd. (Shanghai, China). Ferulic Acid (FA, 98% purity, batch no. 201407116) was purchased from the Shanghai Tongtian Bio-Technology Co., Ltd. (Shanghai, China). Anhydrous ethanol and N,N-dimethylformamide (DMF) were provided by the Shanghai Guangjia Chemicals Co., Ltd. (Shanghai, China). All chemicals used were analytical grade and water was doubly distilled before use.

2.2. Preparation of working fluids and electrospinning

A solvent mixture consisting of 80% ethanol and 20% DMF (v/v) was used as the shell working fluid. A mixed solution composed of 75% (w/v) of shellac and 15% (w/v) FA in ethanol comprised the core fluid. The electrospinning system was formed from a ZDF-2000 power supply (Shanghai Sute Electrical Co., Ltd., Shanghai, China), two KDS 100 syringe pumps (Cole-Parmer®, Vernon Hills, IL, USA), a homemade

concentric spinneret, and a flat piece of cardboard wrapped with aluminum foil used as the fiber collector. Four different types of fibers were prepared with a fixed core fluid flow rate of 2.0 mL/h and a varied shell fluid flow rate (Table 1). The applied voltage and spinneret-to-collector distance were fixed at 12 kV and 15 cm, respectively. The electrospinning processes was recorded using a digital camera (PowerShot A490, Canon, Tokyo, Japan).

Table 1. Details of the electrospinning processes and resultant fibers.

No.	Process	Fluid flow rate (mL/h)		Morphology	Size (μm)
		Shell [a]	Core [b]		
F1	Single fluid	0	2.0	Linear fibers	1.27 ± 0.31
F2	Coaxial	0.2	2.0	Linear fibers	0.87 ± 0.14
F3	Coaxial	0.5	2.0	Linear fibers	0.64 ± 0.15
F4	Coaxial	1.0	2.0	complicated	--

[a] The shell fluid consisted of 80% (v/v) ethanol and 20% (v/v) DMF.

[b] The core fluid consisted of 75% (w/v) shellac and 15% (w/v) of FA in ethanol.

2.3. Morphology

The morphology of the fibers was assessed with a QuantaFEG450 scanning electron microscope (SEM; FEI Corporation, Hillsboro, OR, USA). Samples were subjected to gold sputter-coating under a vacuum to endow them with electrical conductivity prior to measurement. The sizes of the fibers were estimated by measuring them in SEM images at ≥ 100 points, using the ImageJ software (National Institute of Heath, Bethesda, MD, USA). Cross-section fiber samples were prepared by immersing them into liquid nitrogen for 30 minutes and breaking the mats manually.

2.4. Physical form and compatibility of components

Both X-ray diffraction (XRD) and differential scanning calorimetry (DSC) were carried out to investigate the physical form of the components in the fibers. XRD

analyses were performed using a D/Max-BR instrument (Rigaku, Tokyo, Japan) with Cu Kα radiation. Measurements were recorded over the 2θ range 5° to 60° at 40 mV and 30 mA. DSC was conducted using an MDSC 2910 differential scanning calorimeter (TA Instruments Co., New Castle, DE, USA). Samples were heated at a rate of 10 °C/min from 20 °C to 250 °C under a flow of nitrogen (40 mL/min).

Fourier transform infrared (FTIR) spectra were recorded on a Spectrum 100 FTIR spectrometer (PerkinElmer, Waltham, MA, USA) over the range 500 cm^{-1} to 4000 cm^{-1} at a resolution of 2 cm^{-1}.

2.5. In vitro dissolution tests

In accordance with the Chinese Pharmacopoeia (2010 Ed.), *in vitro* dissolution tests were conducted using a paddle method on a RCZ-8A dissolution apparatus (Shanghai Huanghai Medicine Checking Instrument Co., Ltd., Shanghai, China). 0.18 g of the medicated fibers F2 and F3 (equivalent to 30 mg of FA) were first placed in 900 mL of 0.01 N HCl solution for 2h, and later transferred to 900 mL of phosphate buffered saline (PBS, pH 7.0, 0.1 mol/L) for the remainder of the experiment. The temperature of the dissolution media was maintained at 37 ± 1 °C and the paddle rotation speed at 50 rpm. At pre-determined time intervals, 5.0 mL samples were withdrawn and replaced with fresh medium to maintain a constant volume. After filtration and a suitable dilution with PBS, samples were analyzed at λ_{max} = 322 nm using a Lambda 950 UV/vir/NIR spectrophotometer (PerkinElmer, Waltham, MA, USA). The cumulative amount of FA released at each time point was back-calculated from the data obtained against a predetermined calibration curve. Experiments were performed six times, and the results are reported as mean ± S.D.

3. Results and discussion

3.1. Nanofiber design strategy

A schematic explaining the design rationale for the medicated shellac nanofibers prepared in this work is shown in Fig. 1. The concentric spinneret is used as a template to manipulate the two fluids of the electrospinning process. The shell solvent will aid the achievement of a continuous spinning process, ameliorating problems with spinneret clogging and resulting in narrower nanofibers.

The drug-loaded shellac nanofibers can easily be converted into a suitable dosage form for oral administration, for example by incorporation into a capsule. Because shellac is insoluble in acidic conditions, the fibers can protect the loaded active ingredient and hinder release in the stomach. Subsequently, as the pH value of the digestive tract gradually increases, the shellac will absorb water, swell and dissolve, freeing the drug into solution.

Fig. 1.

3.2. Electrospinning

Initially, single-fluid electrospinning was attempted (using the coaxial spinneret, with the flow rate of the shell solvent set to 0 mL/h). The results of this process are depicted in Fig. 2a. Although nanofibers could be produced, a semi-solid substance was found to gradually accumulate on the spinneret, causing clogging (Fig. 2a, inset) and halting the electrospinning process. This blockage had periodically to be manually removed to permit spinning to continue. In contrast, in the modified coaxial

process electrospinning could be run continuously without any user intervention (see Fig. 2b). A compound core-shell Taylor cone could be clearly observed (Fig. 2b, inset).

Fig. 2.

3.3. Morphologies of the raw materials and fibers

Ferulic acid (FA) appears by SEM to be a crystalline powder (Fig. 3a) with a slight yellow color (Fig. 3a inset), whose particles are somewhat less than 50 μm in size. Shellac exists as flakes with smooth surfaces, as shown by the SEM image in Fig. 3b. These have a slight pinkish color (Fig. 3b inset).

After electrospinning, nanoscale fibers are produced: SEM images of these are given in Fig. 3c to 3e. Fibers F1 to F3, produced under shell-to-core fluid flow rate ratios (F) of 0, 0.1 and 0.25 respectively, have linear morphologies without any "beads-on-a-string" phenomena observed. In contrast, when the shell-to-core fluid flow rate ratio was further increased to 0.5, the products exhibited varied morphologies, as illustrated in Fig. 3f. Linear fibers can be found, but so can fibers with beads-on-a-string morphology, together with many clumps and droplets. The excessive shell solvent flow rate used here clearly caused detrimental effects to the products. Thus, a suitable flow rate ratio is key for creating nanofibers with high quality in this setting.

Considering F1 – F3, as the value of F increases, the average diameters (D) of the nanofibers decrease correspondingly (Fig. 3g). Attempts were made to fit the size data using a linear equation (D_1, F_1 and R_1) and exponential equation (D_2, F_2 and R_2).

These gave D_1=1.09-1.87F_1 (R_1=0.9118) and D_2=0.52$F_2^{-0.19}$ (R_2=0.9927) respectively (Fig. 3g): since $R_2 > R_1$, an exponential relationship seems more appropriate. Similar results have previously been reported when surfactant (Triton X-100) or electrolyte (sodium dodecylbenzene sulfonate) solutions were used as shell fluids in coaxial processes to prepare polyacrylonitrile fibers (Yu et al., 2012a; Yu et al., 2012b).

During the coaxial electrospinning processes, the shell solvent system performs two roles. First, it lubricates the core shellac solution. This helps to prevent the formation of semi-solid substances and clogging of the spinneret. Second, the shell solvent surrounds the sticky core solution not only during the formation of the compound Taylor cone, but also in the straight fluid jets and into the bending and whipping regions. It thus helps to keep the core jet in a fluid state for a longer time, allowing it to experience extended electrical drawing. One concern about this double-fluid process, however, is whether the shell solvent causes any solid phase separation to occur. Hence, the cross-sections of F2 and F3 were investigated by SEM (insets of Fig. 3d and 3e, respectively). The fiber cross-sections, just as their surfaces, are very smooth without any visible particles or any other signs of phase separation.

Fig. 3.

3.4. Physical form and component compatibility

The rapid drying which arises during electrospinning (often on a time scale of 10^{-2} s), has rendered it a popular method to generate amorphous dosage forms of poorly water-soluble drugs (Nagy et al., 2015). In order to probe the physical form of the drug in the nanofibers prepared here, we employed X-ray diffraction (XRD) and

differential scanning calorimetry (DSC). Fig. 4a depicts XRD patterns of the raw materials and fibers. The existence of many distinctive Bragg reflections in the FA pattern is consistent with the SEM data (Fig. 3a), and clearly demonstrates that it exists as a crystalline material. In contrast, the pattern for shellac contains only a diffuse halo, as expected since it is known to be an amorphous material. Considering the XRD patterns of the fibers, none of the characteristic FA reflections are visible for F2 or F3, showing that FA exists in an amorphous state in the fibers, having lost its original crystalline form.

The DSC data are entirely consistent with this. The single endothermic response at 174 °C in the DSC thermogram of FA (Fig. 4b) corresponds to melting, confirming the pure FA powder to be a crystalline material. There are no melting events in the DSC curves of shellac, F2, or F3, concurring with the XRD data and proving them to be amorphous.

IR spectra are given in Fig. 4c and chemical structures of the fiber components in Fig. 4c (FA) and 4d (shellac). Both FA and shellac contain–OH and –C=O groups, suggesting that hydrogen bonds can form between them. The characteristic peaks of FA at 1689, 1663 and 1619 cm^{-1} result from the vibration of –C=O groups in the crystal lattice. These vibrations are merged into a single peak at 1698 cm^{-1} in the spectra of F2 and F3. In addition, many peaks in the fingerprint region of the FA spectrum have disappeared in the fibers' spectra. These phenomena taken together verify that FA molecules form composites with shellac through hydrogen bonds, which should improve the components' compatibility and thereby fiber stability.

Fig. 4.

3.5. *In vitro* dissolution tests and drug release mechanism

The results of *in vitro* dissolution tests on F2 and F3 are exhibited in Fig. 5a. As a result of shellac's insolubility in acidic conditions, only a small percentage of FA was released into the dissolution medium during the first two hours at pH 2.0. As is clear from the inset of Fig. 5a, only 8.2% and 9.3% of the embedded FA was released from F2 and F3, respectively. Subsequently, the fibers provided very similar sustained release profiles when they were transferred into the neutral PBS dissolution medium.

The FA release profiles from nanofibers F2 and F3 was analyzed according to the Peppas equation (Peppas, 1985):

$$Q=kt^{n}$$

where Q is the drug accumulative release percentage, t is the release time, k is a rate constant, and n is the release exponent, through which the drug release mechanism can be elucidated. The regressed equations for F2 and F3 between 2 and 8 hours of dissolution are $Q_2=12.9\ t_2^{0.95}$ ($R_2=0.9840$) and $Q_3=14.4t_3^{0.93}$ ($R_3=0.9696$), respectively. The release exponents are 0.95 and 0.93 respectively: slightly larger than 0.89, suggesting that FA release was mainly controlled by the erosion of the polymer matrix.

Given this, one would expect that the shellac must dissolve faster than the encapsulated FA, and thus the dissolution medium should be almost transparent when the FA release approached 100%. However, in fact the dissolution media were still cloudy even after 8 h. To understand this, the F2 dissolution experiments were

repeated, and the fiber mats recovered after various immersion times. The mats were dried under vacuum before being imaged by SEM. The resultant images are given in Fig. 5b to 5g.

Fig. 5.

It can be seen that the fibers are curved and broken in places after immersion in the dissolution media. Their diameters seem to rise, and increasing numbers of nanoparticles appear as dissolution progresses. This is believed to be a result of changes in the shellac molecular conformations as the FA molecules are freed into solution.

A schematic diagram explaining the proposed mechanism of drug release is presented in Fig. 6. When the nanofibers are transferred into the neutral PBS buffer solution, shellac molecules can absorb water and cause the fibers to swell. As a result, the compact structures of the nanofibers gradually expand and unfold. In the medicated fibers, FA molecules are associated with shellac molecules through hydrogen bonds. The fiber swelling and concomitant unfolding of shellac molecules permit the FA molecules to be freed into solution. During this time, the physical entanglements of shellac (marked “A” in Fig. 6) are thought to undergo minimal changes. However, the departure of FA molecules will promote the formation of hydrogen bonds between nearby –OH and –C=O groups within shellac molecules (“B” and “C” in Fig. 6), which in turn result in their crimping. Therefore, the erosion mechanism underlying FA release here is different to the traditional concept where drug release results from the direct dissolution of the carrier. This explains why the

dissolution media were still cloudy even when virtually all the incorporated FA has been freed from the fibers.

Fig. 6.

4. Conclusions

A modified coaxial electrospinning process has been developed for the preparation of ferulic acid (FA)-loaded shellac nanofibers, using a solvent mixture as the shell working fluid. This both helps to ensure a continuous electrospinning process can be implemented, and also can be used to manipulate the fiber diameters. Scanning electron microscopy demonstrated that linear fibers with smooth surfaces and cross-sections were obtained with shell-to-core fluid flow rate ratios of 0.1 and 0.25. FA was incorporated into the fibers in the amorphous physical form, as evidenced by X-ray diffraction and differential scanning calorimetry. IR spectra indicated the existence of hydrogen bonds between the shellac and FA. *In vitro* dissolution tests revealed that less than 10 % of the FA was released in a pH 2 solution, while the majority of the drug was freed over around 8 h in a neutral phosphate buffer. This suggests that the fibers may comprise a useful dosage forms for oral colon-targeted drug delivery. FA is freed from the fibers through an erosion-controlled mechanism, but this is more complex than a simple dissolution of the polymer to free the drug: prior to their dissolution the shellac molecules self-crimped into nanoparticles. The work reported herein comprises a potent strategy for the development of new nanofiber-based drug delivery systems from natural polymers.

Acknowledgements

The authors would like to thank the National Science Foundation of China (grants 51373100, 51373101 and 51173107) and the National Science Foundation of China / Royal Society Exchanges Scheme (Grants 51411130128/IE131748) for financial support.

References

Allen, T.M., Cullis, P.R., 2004. Drug delivery systems: Entering the mainstream. Science 303, 1818-1822.

Baigvera, S., Gavdio, C.D., Lucatelli, E., Kuevda, E., Boieri, M., Mazzanti, B., Bianco, A.,Macchiarini, P., 2014. Electrospun gelatin scaffolds incorporating rat decellularized brain extracellular matrix for neural tissue engineering. Biomaterials 35, 1205-1214.

Balogh, A., Farkas, B., Farago, K., Farkas, A., Wagner, I., Assche, I.V., Verreck, G., Nagy, Z.K., Marosi, G., 2015. Melt-blown and electrospun drug-loaded polymer fiber mats for dissolution enhancement: A comparative study. J. Pharm. Sci. Doi: 10.1002/jps.24399.

Dinis, T.M., Elia, R., Vidal, G., Auffret, A., Kaplan, D. L., Egles, C., 2014. Method to form a fiber/growth factor dual-gradient along electrospun silk for nerve regeneration. ACS Appl. Mater. Interfaces. 6, 16817-16826.

Edwards, A., Javis, D., Hopkins, T., Pixley, S., Bhattarai, N., 2015. Poly(ε-caprolactone)/keratin-based composite nanofibers for biomedical

351 applications. J. Biomed. Mater. Res. B Appl. Biomater. 103, 21-30.
352 Farokhzad, O. C., 2008. Nanotechnology for drug delivery: the perfect partnership.
353 Expert Opin. Drug Del. 5, 927-929.
354 Henning, S., Leick, S., Kott, M., Rehage, H., Suter, D., 2012. Sealing liquid-filled
355 pectinate capsules with a shellac coating. J. Microencapsul. 29, 147-155.
356 Hubbell, J.A., Chikoti, A., 2012. Nanomaterials for drug delivery. Science 337,
357 303-305.
358 Kai, D., Liow, S.S., Loh, X.J., 2014. Biodegradable polymers for electrospinning:
359 Towards biomedical applications. Mater. Sci. Eng. C 45, 659-670.
360 Limmatvapirat, S., Limmatvapirat, C., Puttipipatkhachorn, S., Nuntanid, J.,
361 Luangtana-anan, M., 2007. Enhanced enteric properties and stability of shellac
362 films through composite salts formation. Eur. J. Pharm. Biopharm. 67, 690-698.
363 Limmatvapirat, S., Panchapornpon, D., Limmatvapirat, C., Nunthanid, J.,
364 Luangtana-Anan, M., Puttipipatkhachorn, S., 2008. Formation of shellac succinate
365 having improved enteric film properties through dry media reaction. Eur. J.
366 Pharm. Biopharm. 70, 335-344.
367 Lin, H.Y., Chen, H.H., Chang, S.H., Ni, T.S., 2013. Pectin-chitosan-PVA nanofibrous
368 scaffold made by electrospinning and its potential use as a skin tissue scaffold. J.
369 Biomater. Sci. Polym. Ed. 24, 470-484.
370 Liu, Z., Jiao, Y., Wang, Y., Zhou, C., Zhang, Z., 2008. Polysaccharides-based
371 nanoparticles as drug delivery systems. Adv. Drug Del. Rev. 60, 1650-1662.
372 Ma, G., Fang, D., Liu, Y., Zhu, X., Nie, J., 2012. Electrospun sodium

alginate/poly(ethylene oxide) core–shell nanofibers scaffolds potential for tissue engineering applications. Carbohydr. Polym. 87, 737-743.

Merisko-Liversidge, E., Liversidge, G.G., 2011. Nanosizing for oral and parenteral drug delivery: A perspective on formulating poorly-water soluble compounds using wet media milling technology. Adv. Drug Del. Rev. 63, 427-440.

Mogosanu, G.D., Mihai Grumezescu, A., Chifiriuc, M.C., 2014. Keratin-based biomaterials for biomedical applications. Curr. Drug Target. 15, 518-530.

Nagy, Z.K., Balogh, A., Démuth, B., Pataki, H., Vigh, T., Szabó, B., Molnár, K., Schmidt, B.T., Horák, P., Marosi, G., Verreck, G., Assche, I.V., Brewster M.E., 2015. High speed electrospinning for scaled-up production of amorphous solid dispersion of itraconazole. Int. J. Pharm. 480, 137-142.

Paaver, U., Heinämäki, J., Laidmäe, I., Lust, A., Kozlova, J., Sillaste, E., Kirsimäe, K., Veski, P., Kogermann, K., 2015. Electrospun nanofibers as a potential controlled-release solid dispersion system for poorly water-soluble drugs. Int. J. Pharm. 479, 252-260.

Peppas, N.A., 1985. Analysis of Fickian and non-Fickian drug release from polymers. Pharm. Acta Hel. 60, 110-111.

Pouton, C.W., Porter, C.J.H., 2008. Formulation of lipid-based delivery systems for oral administration: Materials, methods and strategies. Adv. Drug Del. Rev. 60,625-637.

Rachmawati, H., Mudhakir, D., Kusuma, J., 2012. Combination of inulin-shellac as a unique coating formulation for design of colonic delivery dosage form of

ibuprofen. J. Res. Pharm. Sci. 3, 17-23.

Ravi, V., Siddaramaiah, Kumar, T.M.P., 2008. Influence of natural polymer coating on novel colon targeting drug delivery system. J. Mater. Sci. Mater. Med. 19, 2131-2136.

Sridhar, R., Lakshminarayanan, R., Madhaiyan, K., Barathi, V.A., Limh, K.H.C., Ramakrishna, S., 2015. Electrosprayed nanoparticles and electrospun nanofibers based on natural materials: applications in tissue regeneration, drug delivery and pharmaceuticals. Chem. Soc. Rev. 44, 790-814.

Sun, B., Long, Y.Z., Zhang, H.D., Li, M.M., Duvail, J.L., Jiang, X.Y., Yin, H.L., 2014. Advances in three-dimensional nanofibrous macrostructures via electrospinning. Prog. Polym. Sci. 39, 862-890.

Vats, A., Pathak, K., 2013. Exploiting microspheres as a therapeutic proficient doer for colon delivery: a review. Expert Opin. Drug Del. 10, 545-557.

Vrbata, P., Berka, P., Stránská, D., Doležal, P., Lázníček, M., 2014. Electrospinning of diosmin from aqueous solutions for improved dissolution and oral absorption. Int. J. Pharm. 473, 407-413.

Yu, D.G., Chatterton, N.P., Yang, J.H., Wang, X., Liao, Y.Z., 2012a. Coaxial Electrospinning with Triton X-100 Solutions as Sheath Fluids for Preparing PAN Nanofibers. Macromol. Mater. Eng. 297, 395-401.

Yu, D.G., Wang, X., Li, X.Y., Chian, W.,Li, Y., Liao, Y.Z., 2013. Electrospun biphasic drug release polyvinylpyrrolidone/ethyl cellulose core/sheath nanofibers. Acta Biomater. 9, 5665-5672.

Yu, D.G., Williams, G.R., Gao, L.D., Bligh, S.W.A., Yang, J.H., Wang, X., 2012b. Coaxial electrospinning with sodium dodecylbenzene sulfonate solution for high quality polyacrylonitrile nanofibers. Colloid. Surface A 396, 161-168.

Zhang, S., Chen, L., Jiang, Y., Cai, Y., Xu, G., Tang, T., Zhang, W., Wang, L., Ji, J., Shi, P., Ouyang, H.W., 2013. Bi-layer collagen/microporous electrospun nanofiber scaffold improves the osteochondral regeneration. Acta Biomater. 9, 7236-7247.

Figures and table legends

Fig. 1. A schematic illustrating the strategy underlying the design of the medicated shellac nanofibers prepared in this work.

Fig. 2. Photographs of the electrospinning of FA-loaded shellac nanofibers using (a) single-fluid and (b) coaxial electrospinning. The inset in (a) shows clogging of the spinneret and that in (b) the Taylor cone observed during the coaxial process with shell and core fluid flow rates of 0.5 and 2 mL/h, respectively.

Fig. 3. SEM images of the raw materials and nanofibers. (a) FA particles (photograph as inset); (b) a cross-section of a shellac sheet (photograph as inset); (c) F1; (d) F2; (e) F3; (f) F4; and, (g) the influence of shell-to-core fluid flow ratio on fiber diameter. The insets in (d) and (e) show the fiber cross-sections.

Fig. 4. Physical form and component compatibility data. (a) XRD patterns; (b) DSC thermograms; (c) IR spectra; and, (d) the molecular structure of shellac.

Fig. 5. The results of *in vitro* dissolution tests. The FA release profiles are given in (a),

together with SEM images of F2 after (b) and (c) 3h; (d) and (e) 5h; and, (f) and (g) 7h of dissolution

Fig. 6. A schematic diagram of the proposed drug release mechanism.

Table 1. Details of the electrospinning processes and resultant nanofibers.

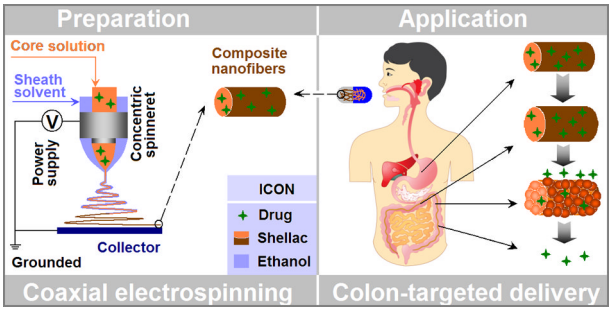

Fig.1.

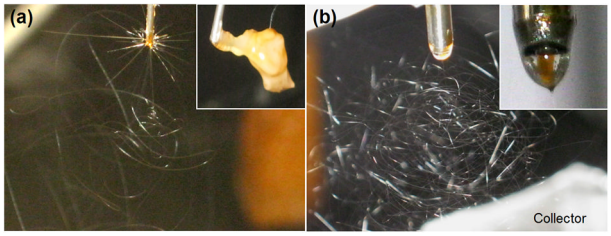

Fig. 2.

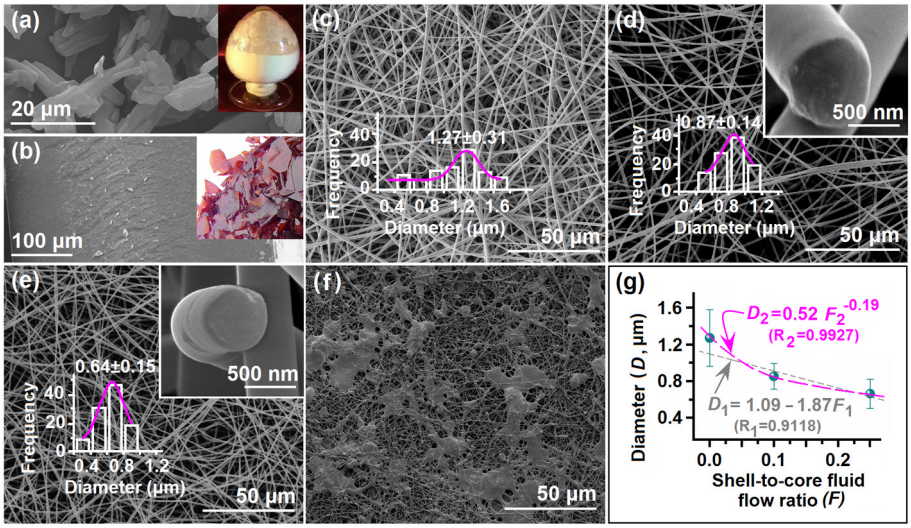

Fig. 3.

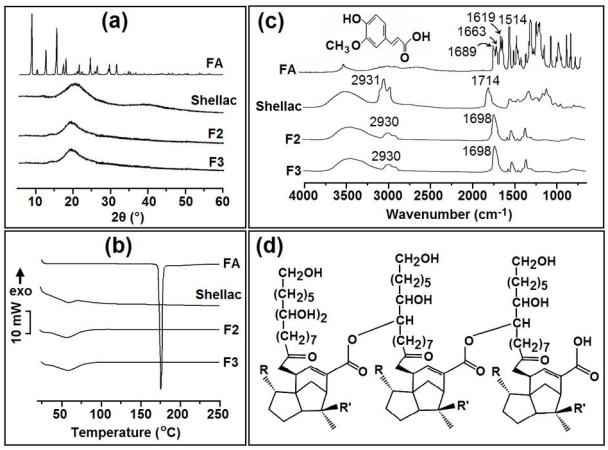

Fig. 4.

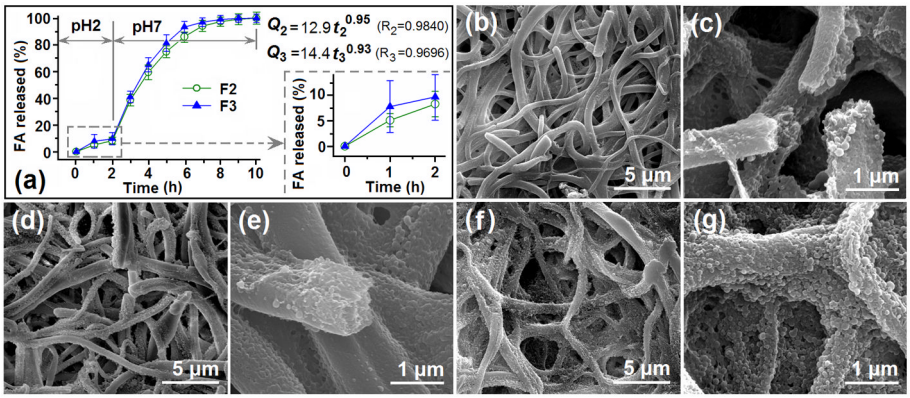

Fig. 5.

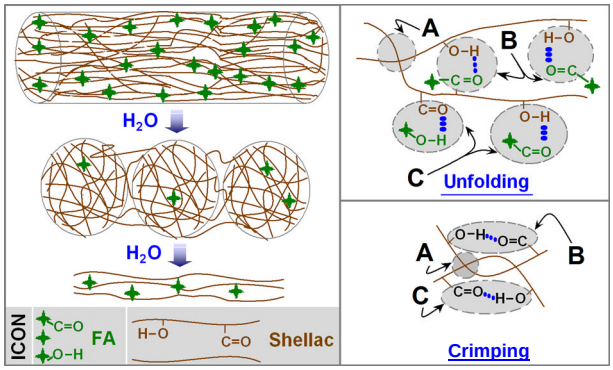

Fig. 6.

Graphical abstract

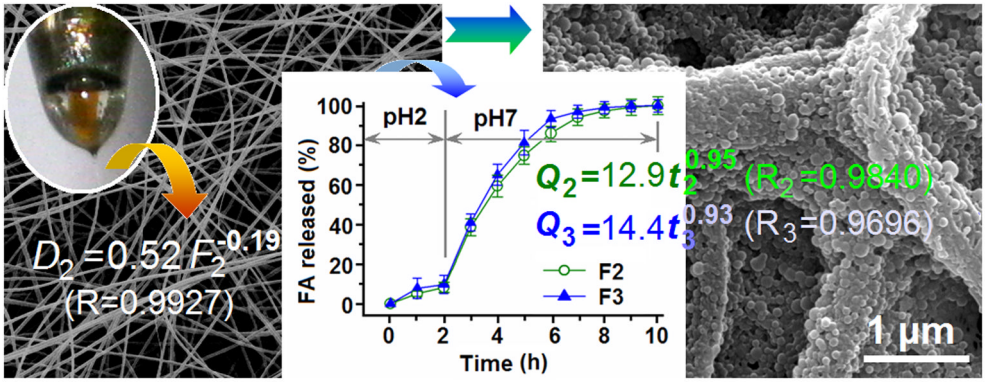

(5 cm ×13 cm)